Anomalous incommensurability and embryonic fluctuations in lead phosphate $Pb_3(PO_4)_2$

J. M. Kiat
Laboratoire de Chimie-Physique du Solide, Ecole Centrale, 92295 Chatenay-Malabry, France and Laboratorie Léon Brillouin, Centre d'Etudes Nucléaires de Saclay, 91191 Gif-sur-Yvette, France

G. Calvarin
Laboratoire de Chimie-Physique du Solide, Ecole Centrale, 92295 Chatenay-Malabry, France

Y. Yamada
Institute for Solid State Physics, The University of Tokyo, 7-22-1 Roppongi, Minato-ku, Tokyo 106, Japan
(Received 7 October 1992; revised manuscript received 16 February 1993)

We report the results of precise x-ray- and neutron-scattering experiments on lead phosphate in the critical-temperature region of the ferroelastic transition. These results show the existence of anomalous incommensurate satellite reflections above T_c, where the incommensurability changes from one Brillouin zone to another. It is shown that the incommensurate satellites are located at the commensurate reciprocal-lattice points of the monoclinic cell, which is stabilized below T_c. Similar phenomena are known to occur in the precursor regime of the martensitic phase transitions of metals and alloys such as Ti-Ni. The present investigation provides an observation of an anomalous incommensurability in a nonmetallic compound. The observed results are interpreted in terms of embryonic fluctuations, which are theoretically predicted to exist at a first-order phase-transition point when there is strong coupling between the order parameter and the bulk strain.

I. INTRODUCTION

In the last years, the precursor phenomena of martensitic transformation of metals and alloys have been the subject of numerous studies because they are considered to provide an important key to understand the mechanism of martensitic transformation. One of the precursor phenomena is the appearance of anomalous satellite reflections at noncommensurate positions observed in the diffraction experiments. The positions of satellites exhibit peculiar symmetry properties in the reciprocal space which preclude any interpretation based on a simple incommensurate structure model. That is, the incommensurability $\delta\mathbf{Q}$ changes from one Brillouin zone to another, and does not satisfy the inversion symmetry around the Brillouin-zone center.

Salamon, Meichle, and Wayman[1] first pointed out that these anomalous diffraction patterns could be understood if one assumes that the satellites are at the commensurate reciprocal lattice points of the low-temperature (martensite) phase, while the fundamental Bragg reflections are at the commensurate positions of the high-temperature (austenite) phase. They called this reciprocal lattice a "ghost lattice"; the satellites are the "ghost" because they appear before the transition actually takes place.

A possible microscopic model to explain these anomalies has been developed by Yamada and coworkers. They succeeded in explaining the ghost lattice effect of Ti-Ni and Au-Cd (Refs. 2 and 3) using a specific lattice-dynamical model called modulated lattice relaxation (MLR). More recently Fuchizaki and Yamada[4] developed a phenomenological theory which shows that, in principle, any crystal undergoing a first-order phase transition could display such anomalous incommensurability if a strong coupling between the intrinsic order parameter and the strains exists: Their result is no more restricted by a microscopic lattice-dynamical model as previously assumed in the case of Ti-Ni and Au-Cd.

Up to now, no experimental observation of such an effect in nonmetallic materials has been carried out. In this article we report experimental results showing the existence of the ghost lattice anomalies in a nonmetallic compound, lead phosphate, above its ferroelastic transition temperature.

Lead phosphate $Pb_3P_2O_8$ [or $Pb_3(PO_4)_2$] undergoes a first-order ferroelastic phase transition at $T_c = 180\,^{\circ}C$ from a high-temperature (HT) rhombohedral phase to a low-temperature (LT) monoclinic phase. This transition was for a long time known as one of the best textbook examples of ferroelastic phase transition because it was the first reported purely ferroelastic material (no coupling with any other properties such as ferroelectricity). The space group of the HT phase is $R\bar{3}m$, the space group of the LT phase was reported to be $C2/c$ but the real symmetry is in fact $C2$ as recent experiments have shown.[5] The ferroelastic transition occurs by the condensation of a phonon mode at the L point of the rhombohedral Brillouin zone (the zone boundary along the $\langle 100 \rangle$ direction).[6] Therefore, besides the monoclinic bulk deformation, the unit cell is doubled and superstructure reflections appear as the transition takes place.

However, experimental results on x-ray diffraction[6] and neutron diffraction[7,8] have shown that weak superstructure reflections persist above the transition temperature. These results, together with other experimental results on Raman scattering[9] and electron paramagnetic

resonance measurements,[10] were interpreted by assuming that small embryo regions of the LT phase persist above T_c in the HT phase, in the temperature range 180–300 °C. This interpretation, however, is still controversial because the fundamental Bragg peaks do not show splitting corresponding to the inclusion of monoclinic regions in the rhombohedral matrix (two phase coexistence). Moreover, a debate exists about the static or the dynamic nature of these embroys: On one hand, inelastic neutron-scattering,[8] electron-diffraction,[11] Mossbauer γ-ray-scattering,[12] and Raman-scattering[9] results could be satisfactorily interpreted by assuming that the embryos exist for a short time in one orientation and then flip to one of the other two orientations; on the other hand, observations of domainlike structure above T_c (Ref. 13) in pure lead phosphate by electron microscopy and the existence of a central peak in neutron spectra in mixed compound $Pb_3P_{2x}V_{2(1-x)}O_8$ with $x=0.95$,[14] were consistent with the persistence of a static monoclinic region inside the HT phase.

We have tried to clarify this situation by performing a precise reinvestigation of the critical regime of lead phosphate. Preliminary investigations were made by carrying out a precise measurement of the temperature dependence of the lattice parameters, using an x-ray high accuracy diffractometer on single crystals. An overall examination of the Bragg and superstructure reflections was also performed in both LT and HT phases using an x-ray precession camera. Then, some superstructure reflections were selected and $\theta/2\theta$ scans were carried out with changing temperature: anomalies in the temperature dependence of positions, widths, and intensities were evidenced above T_c. A further step was achieved by performing a mapping in reciprocal space of some of these superstructure reflections as well as of some Bragg reflections, below and above the critical temperature; for this we used x-ray and neutron diffraction in order to get comparative as well as complementary information. Finally an energy analysis of the superstructure reflections was carried out with a neutron triple-axis spectrometer.

II. EXPERIMENTAL RESULTS

In order to make comparisons much easier between LT and HT phases a common monoclinic indexing is used throughout this paper. The rhombohedral lattice can be considered as a face-centered (F) monoclinic lattice with additional algebraic relationships ($c=b\sqrt{3}=3a\cos\beta$) between the lattice parameters.

A. Temperature dependence of the lattice parameters

Up to now the temperature dependence of the cell parameters of lead phosphate on a single crystal was only known from x-ray photograph studies.[6,15] In order to get more accurate results we have performed an experiment using a high-resolution x-ray two-axis diffractometer (Bragg-Brentano reflection geometry) with the Cu $K\alpha 1$ monochromatic radiation of a 18-kw Rigaku rotating anode; a Riguku furnace was used with stability of 1 K and precision of 2 K. The variations of the cell parameters a, b, c, β were determined with single crystals by recording the temperature dependence of four Bragg peaks 8 0 0, 0 4 0, $-1\ -1\ 3$, and $15\ -1\ -3$.

Figure 1 shows the temperature dependence of the unit-cell volume V and of the cell parameters b, c, $a\sin\beta$ (the latter parameter corresponds to the unique axis of the HT phase). As temperature is increased a strong decrease of the b parameter is observed in the monoclinic phase in contrast to the other parameters, which show ordinary positive thermal-expansion coefficient. At $T_c=180$ °C all the parameters exhibit a discontinuity. Within the rhombohedral phase the b parameter recovers a positive thermal expansion; moreover at about 300 °C a change in the slopes of $b(T)$, $c(T)$, and $a\sin\beta(T)$ curves is detected. These temperature dependences of parameters result in a variation of the volume which is rather extraordinary: in the LT phase the volume thermal-expansion coefficient is negative as the b contribution is predominant; at 6 K the volume is still larger than at room-temperature (the corresponding value is not represented on figure). At T_c there is a discontinuous decrease and in the rhombohedral HT phase the volume increases in such a way that the room-temperature value is recovered at about 260 °C. A change in the slope of the $V(T)$ curve is also observed at 300 °C.

B. Study of the superstructure reflections

The lattice of the HT phase is face centered in the monoclinic description. Thus, the Miller's indices h,k,l

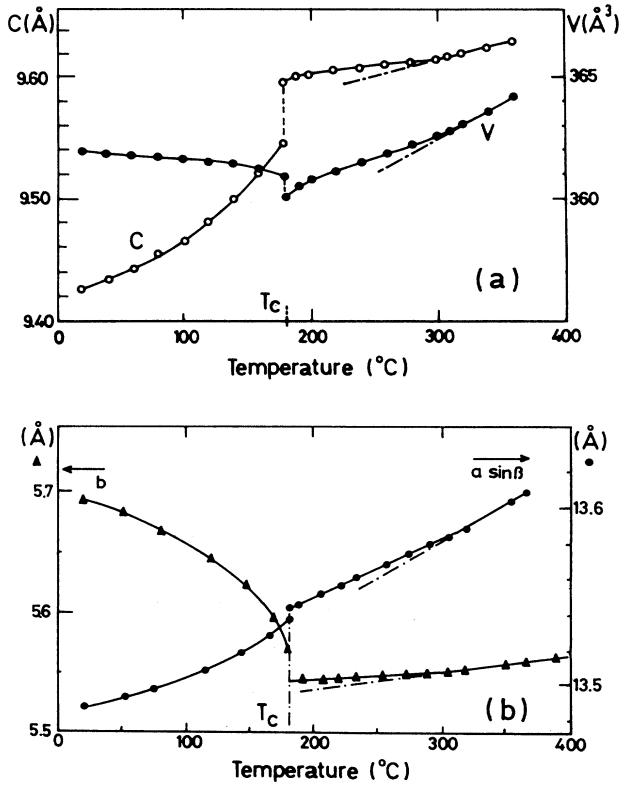

FIG. 1. Temperature dependence of cell parameters; a common monoclinic cell for both LT and HT phases was used; V is for the volume of the unit cell.

have the same parity. The phase transition occurs by the condensation of a phonon mode at the L point of the rhombohedral Brillouin zone ($\mathbf{q}=1/2\mathbf{b}_r^*=\mathbf{c}^*$).[6] Therefore, in the LT phase a pair of satellite reflections appear around each h,k,l reflection, which are identified to be the superstructure reflections indexed as $h,k,l\pm1$.

1. X-ray precession results

Precession photographs were obtained using a Burger camera (Huber apparatus) with the Cu $K\alpha1$ radiation (graphite monochromator) of a rotating 12-kW anode. Photographs of the HT phase were taken with a Huber heating head (stability of 1°). A single crystal with 100 μm width was cut perpendicularly to the c monoclinic axis. We have recorded the $h,k,0$ reciprocal plane (Fig. 2) which contains, depending on the temperature, two types of peaks: the Bragg peaks (h and k even) of the LT and HT phases, and the superstructure peaks (h and k odd) of the LT phase.

At room temperature we observed the splitting of some Bragg peaks, which reveals the multidomain character of the sample: Due to breaking of the rhombohedral threefold symmetry, three types of domains coexist sharing the common a^* axis. On the diffraction pattern this results in the observation of reflections belonging to other domains at a slightly different 2θ position. For more details about this problem see Ref. 6. Some strong superstructure reflections are observed, for instance the 3 1 0, 3 3 0, and 3 5 0 reflections.

In the HT phase the splitting of Bragg peaks is no more detected in the photographs, which is consistent with the recovery of the rhombohedral symmetry. Moreover, whereas the experimental setup is not optimized for diffuse scattering studies, the persistence of intensity is observed around the positions with mixed parity: 3 1 0, 3 3 0, 3 5 0, 5 3 0, 5 5 0, 9 3 0, and 9 5 0 as schematically represented in Fig. 2. These diffuse peaks are much broader than the corresponding superstructure peaks in the LT phase, with a very anisotropic shape where the principal axis of elongation is along the a^* axis, as it has already been reported.[7] The width along this direction is at least two or three times larger than along the b^* axis.

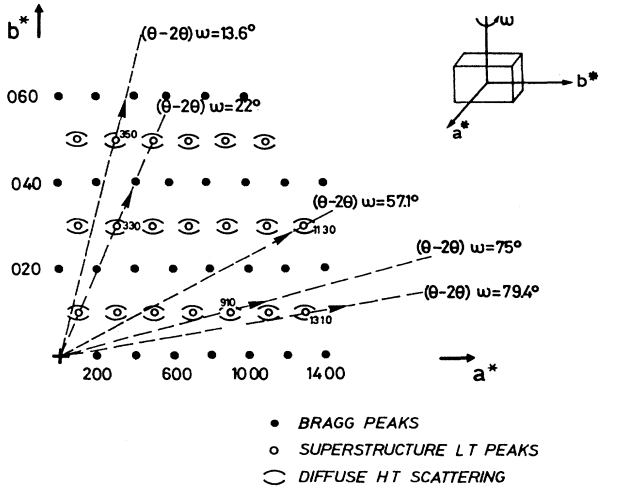

FIG. 2. Schematic representation of the $h,k,0$ plane; the direction of the $\theta/2\theta$ scans performed in the x-ray goniometric study is also indicated by dashed lines.

2. X-ray goniometry results

We have performed $\theta/2\theta$ scans of the superstructure peaks 3 3 0, 3 5 0, 9 1 0, 13 1 0, and 11 3 0, at various temperatures, with the same equipment used for the measurement of the cell parameters. A sample of $0.5\times5\times10$ mm^3 with faces perpendicular to b, c, and $a\sin\beta$ was used. The corresponding directions of scans are indicated in Fig. 2. Typical $\theta/2\theta$ scans are shown in Fig. 3 for the 9 1 0 reflection.

The variation of the intensity and of the full width at half maximum (FWHM) of all these lines have globally the same characteristic features. The curve of the integrated intensity versus temperature is plotted in Fig. 4 for the 9 1 0 peak. On heating the intensity decreased continuously up to T_c where a discontinuous jump is observed. However, above T_c some intensity is still observed, in some cases up to 310 °C. As previously pointed out, these reflections should be absent in the space group $R\bar{3}m$. At room temperature the FWHM (Fig. 5) of the superstructure peaks shows values of the same magnitude

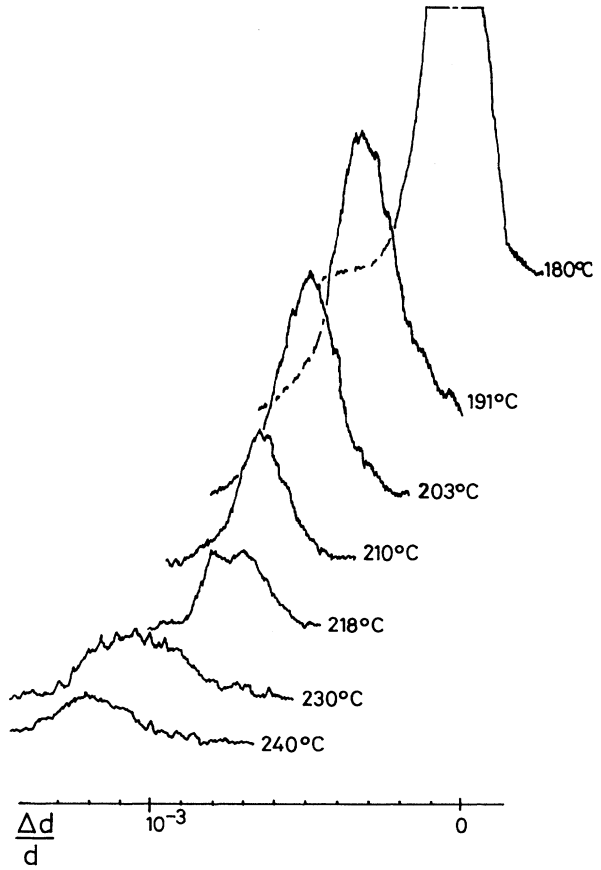

FIG. 3. Intensity profiles of $\theta/2\theta$ scans of the diffuse precursor reflection 9 1 0 shown for some temperatures above T_c.

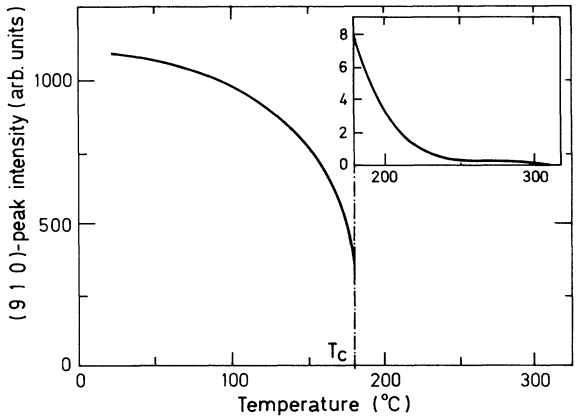

FIG. 4. Integrated intensity of the 9 1 0 reflection vs temperature. The inset shows that the superstructure (precursor) reflection persists up to 300 °C.

as the Bragg peaks and they remain constant up to T_c. At T_c a discontinuous increase is observed followed by a slight decrease, then they strongly increase.

The existence of these prohibited reflections above T_c would mean that, while the sample is kept in thermal equilibrium at $T > T_c$, the crystal prepared itself for the phase transition before it actually takes place. In this context, these residual superstructure reflections are called the "precursor reflections" hereafter.

In Fig. 6, the d spacings for the 9 1 0 and 3 3 0 reflections have been plotted using the formula

$$d = \lambda / 2 \sin\theta \ . \tag{1}$$

One notices that the experimental d spacings do not show any discontinuities at T_c, whereas the transition is clearly first order as evidenced by the discontinuous jump of the cell parameters (Fig. 1). This implies that there must be some discrepancies between the observed d spacings using Eq. (1) and those calculated from the unit-cell parameters by the formula

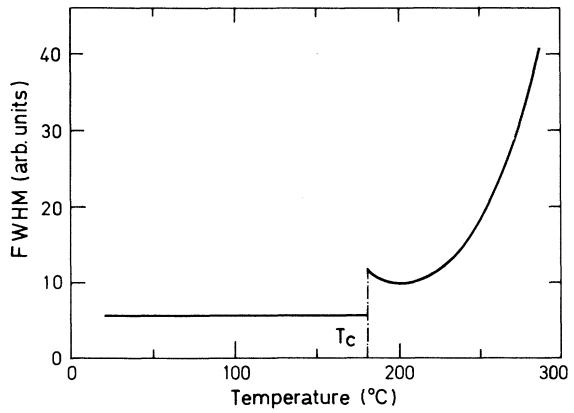

FIG. 5. Typical temperature variation of FWHM of the superstructure (precursor) reflections. Below T_c it remains constant, with the same magnitude as that of fundamental Bragg reflections.

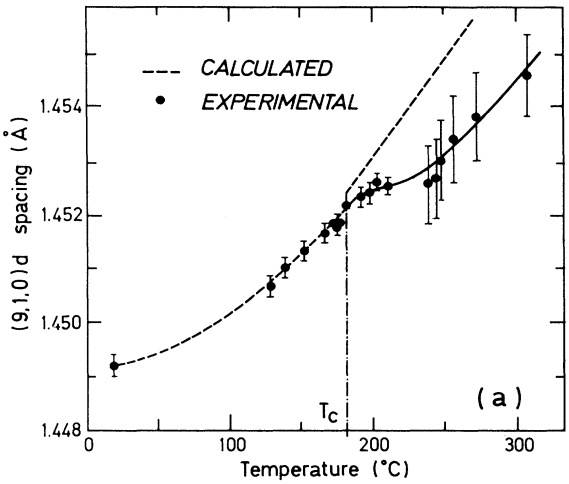

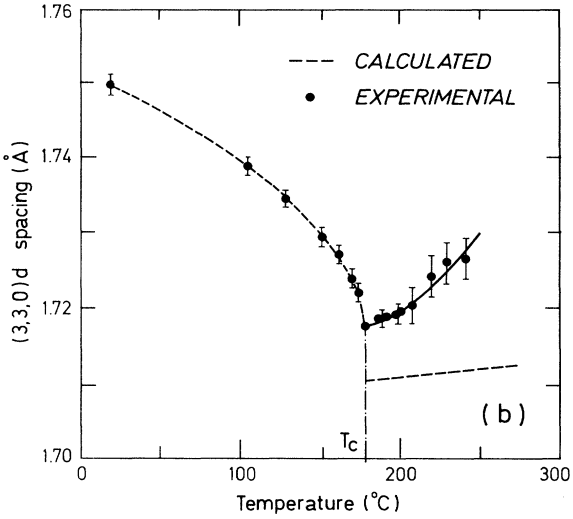

FIG. 6. Temperature dependence of d spacings of the superstructure precursor reflections 9 1 0 and 3 3 0; the dotted lines are calculated values from the cell parameters determined by the temperature variation of Bragg peaks.

$$d_{h,k,0} = [(h/a \sin\beta)^2 + (k/b)^2]^{1/2} \ . \tag{2}$$

The "calculated" d spacings with Eq. (2) are also included in Fig. 6 (dashed lines). Up to T_c a good agreement between the experimental and the calculated d spacings is observed. However, above T_c these values become definitely different, and the disagreement becomes more enhanced as the temperature is increased. That is, the peak positions of the precursor reflections are incommensurate to the fundamental rhombohedral lattice.

3. *X-ray and neutron mapping results*

The $\theta/2\theta$ scans revealed that the precursor reflections are shifted from the commensurate position above T_c. In order to get detailed information on these shifts in the reciprocal space, we have performed complete mapping of

intensity distribution in the $h\ k\ 0$ plane of these precursor reflections, as Shapiro *et al.* did in the case of Ti-Ni(Fe).[16] Both x-ray and neutron experiments were performed in order to get complementary information on as large as possible number of reflections and eventually to detect possible differences between the bulk and the surface of the sample. The diffraction geometry used in the neutron experiments also provided information outside the $h\ k\ 0$ plane. For the x-ray experiments we used the same experimental setup as described above (Bragg-Brentano reflection geometry), and the mappings were performed by automatic ω scans at different 2θ positions. In that case the FWHM of the 0 4 0 Bragg peak was $0.08a^*$ and $0.08b^*$. For the neutron experiments we performed Q scan with the neutron four-circle diffractometer installed at the Orphée reactor (CEN Saclay) ($\lambda=0.831$ Å) with an erbium filter (attenuation 0.7×10^{-3}) on a single domain crystal of dimensions $12\times10\times7$ mm^3; for the 0 4 0 Bragg peak the FWHM was $0.10a^*$ and $0.10b^*$.

In Figs. 7, 8, and 9 the x-ray mappings (at $T=T_c+4°$) of the Bragg peak 0 4 0 and of the precursor reflections 9 1 0 and 3 5 0 are plotted. The anisotropic distribution of equi-intensity contours results from a combination of instrumental effects (mainly strong vertical divergency, as we were obliged to work with very large opening slit due to the weak intensity of the superstructure lines, and spectral distribution), anisotropic mosaic spread due to the layered structure, and intrinsic effects as observed in the precession photograph: In this experiment these effects are strongly Q dependent and are difficult to separate.

As seen in Fig. 7, the 0 4 0 Bragg peak is sitting at the exact commensurate position. On the other hand, the precursor peaks (Figs. 8 and 9) show incommensurate shifts but these shifts change throughout the reciprocal lattice. That is, the δ value is dependent on the Miller indices in directions as well as in magnitudes. The overall shift pattern of precursor reflections in ($h\ k\ 0$) plane is schematically represented in Fig. 10. This effect is discussed in the last paragraph.

Figure 11 gives a schematic view of neutron mappings of Bragg peaks 0 4 0, 8 0 0, 2 2 0, 4 4 0, and of precursor reflections 3 3 0, 3 5 0, and 3 7 0 observed above T_c. The shape of the intensity distribution of Bragg peaks is due to instrumental effects and thus is different depending on their location in the a^*-b^* reciprocal space.

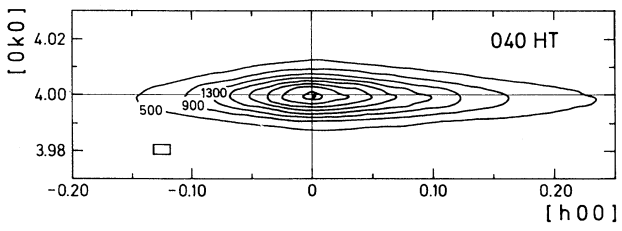

FIG. 7. X-ray mapping of Bragg peak 0 4 0 at $T_c+4°$; the observed peak position (indicated by the black circle) is commensurate to the reciprocal lattice point of the high-temperature phase structure. The rectangular box is the estimated error on the location of the maximum of the map.

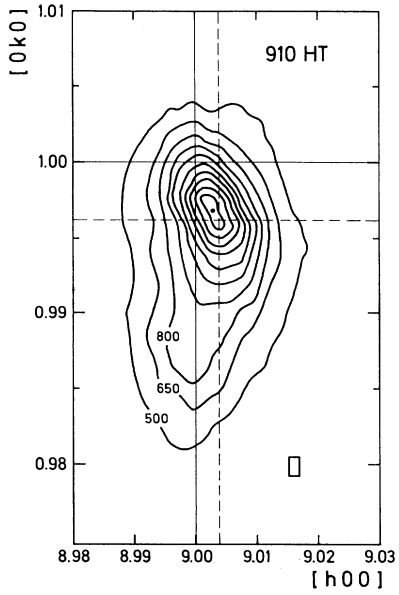

FIG. 8. X-ray mapping of precursor reflection 9 1 0 at $T_c+4°$; the cross point of the dashed lines indicates 9 1 0 position calculated from the low-temperature cell parameters. The rectangular box is the estimated error on the location of the maximum of the map. Within this error the observed peak (black circle) is commensurate to the reciprocal lattice point of the *low-temperature* structure.

Concerning the precursor reflections the most prominent fact is the observation of a splitting of peaks that we never observed in the x-ray experiments. These splittings were detected by ω scans on the whole set of superstructure reflections that we have studied: 3 1 0, 3 3 0, 3 5 0, 3 7 0, 3 9 0, 9 3 0, 9 7 0, 1 3 5 0, 1 9 5 0, $-1\ 1\ 2$, and 3 5 2. Notice the splitting is not due to the two-phase coexistence because it was not observed in any of the fundamental Bragg peaks. For each doublet, one of the peaks seems to be located at the commensurate position and the other is located at an incommensurate position. In the

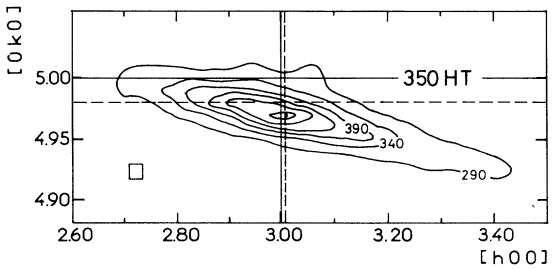

FIG. 9. X-ray mapping of precursor reflection 3 5 0 at $T_c+4°$; the cross point of the dashed lines indicates 3 5 0 position calculated from the low-temperature cell parameters. The rectangular box is the estimated error on the location of the maximum of the map. Within this error the observed peak (black circle) is commensurate to the reciprocal lattice point of the *low-temperature* structure.

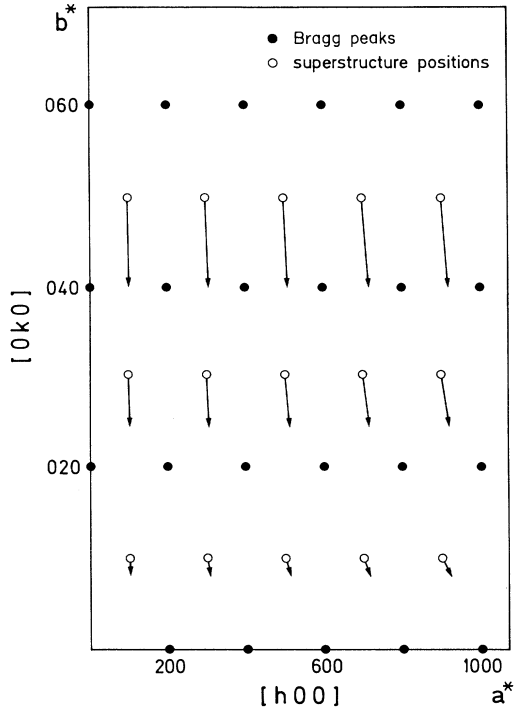

FIG. 10. Schematic representation of the $h,k,0$ plane showing the direction and the magnitude (enlarged) of the shift of the precursor reflections. The shifted positions coincide with the reciprocal lattice points of the low-temperature phase.

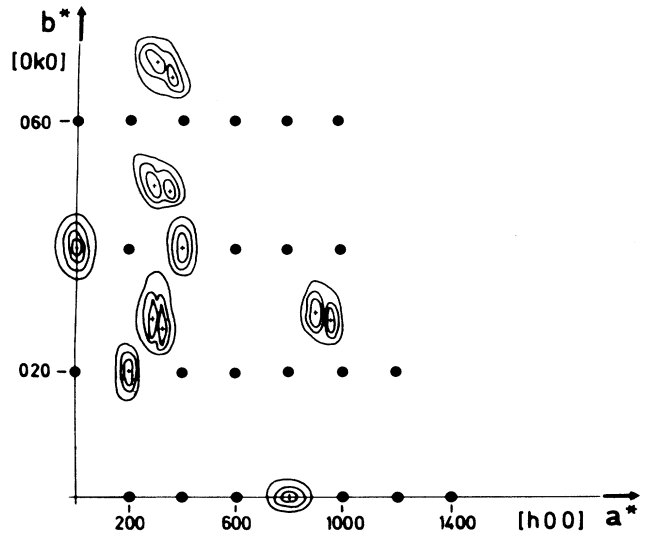

FIG. 11. Schematic representation of the mappings observed during the neutron experiment. Only the precursor reflections show splitting into doublet. The scale of the splittings are enlarged by factor of about 10.

present neutron experiment, however, the precision of the position determination is not sufficient to make quantitative measurement of the incommensurability and of its Q dependence. Each component of the doublet has a much broader width along the a^* direction than along the b^* direction. A scan along the c^* direction shows no broadening. On increasing the temperature, the commensurate peak first disappears and afterwards the incommensurate peak diminishes.

The inelasticity of the neutron spectra of precursor reflections has already been extensively investigated.[7,8] However, since defects and internal strain have been suspected to cause changes in the dynamical behavior of lead phosphate,[12,13] we have tried to check the inelastic nature of precursor reflections on our sample. Using a triple-axis spectrometer on a cold source ($k=2.662$ Å^{-1}) with a pyrolitic graphite filter (attenuation better than 5×10^{-3}), we have performed q scans and energy scan of some Bragg peaks at points 2 2 0, 0 4 0, and 4 0 0 and of the precursor peaks 3 3 0 at $T=T_c+5°$. For the Bragg peaks we obtained instrumental resolution limited distribution in the Q space and an energy distribution with a Gaussian profile having 0.04 THz in FWHM. In the case of the 3 3 0 reflection the Q scans show a splitting into doublet. We have performed energy scans at both maxima of this doublet. In each case we obtained Gaussian profiles with typically 0.20 THz in FWHM. As the calculated value is of the same order (about 0.19 THz) it is difficult to decide the elastic or the quasielastic nature of the precursor peaks.

III. SUMMARY AND DISCUSSION

This study has shown in accordance with other previous results that the ferroelastic phase transition of lead phosphate possesses the following characteristics.

(1) It is first order with discontinuous jumps in the lattice parameters at the critical temperature $T_c=180$ °C.

(2) Above T_c the superstructure reflections of the monoclinic phase persist as precursor reflections in the form of cigar-shaped (along a^*) diffuse peaks up to 300 °C.

(3) Around the temperature where the precursor reflections disappear, changes in the slope of the temperature dependence of lattice parameters are also observed.

The main results of this study are associated with the precise determination of positions of precursor reflections. Clearly the peak positions above T_c are shifted from their commensurate positions in such a way that the incommensurability changes from one Brillouin zone to another.

This anomalous incommensurability rules out the possibility to explain the structural characteristic, at $T>T_c$, by an ordinary modulated structure model. Similar anomalies have already been reported in some metals and alloys undergoing the martensitic transformation: in particular in the ω phase of some Zr-Nb alloys,[17] in the α phase of uranium,[18,19] and in the β phase of Ti-Ni(Fe).[16] For β-Ti-Ni(Fe) extensive studies of the diffraction pattern were performed. It was pointed out that the diffraction pattern could be systematically reproduced by assuming that the satellite precursor peaks "foresee" the LT structure and are sitting at the commensurate positions of the LT lattice, whereas the fundamental Bragg reflections construct the HT reciprocal lattice. This behavior of the diffraction pattern is called a ghost lattice

effect and is considered to be a signature of the premartensitic regime.

Assuming the relevance of these considerations to our problem, we can predict the positions of precursor peaks in the $hk0$ zone above T_c. On the x-ray mappings of 9 1 0 and 3 5 0 lines (Figs. 8 and 9), we have indicated the positions (cross point of the dashed lines at 9.0039 0.9961 and 3.0016 4.9805) calculated with the LT lattice parameters (at 179 °C $a\sin\beta = 13.5368$ Å and $b = 5.5665$ Å). It is clearly seen that within the experimental error the observed peak positions (9.0029 ± 0.0016 0.9969 ± 0.0012 and 3.0072 ± 0.025 4.9696 ± 0.013) agree with the commensurate positions *of the* LT *phase.* Using the LT lattice parameters we can systematically index the precursor peaks, and thus understand the dependence of the incommensurate shifts on the Miller indices in direction as well as in magnitude. The overall shift pattern of the precursor reflections from their commensurate positions of the HT phase is shown in Fig. 10: The components of the shifts along a^* and b^* are proportional to the Miller indices. This clearly demonstrates the ghost lattice effect of $Pb_3(PO_4)_2$.

The physical origin of the ghost lattice behavior has been elucidated by Yamada and coworkers. In the earlier works, a specific microscopic model called MLR (modulated lattice relaxation) was developed,[3] which is applicable to bcc alloys. It is based on the following two assumptions: (i) the existence of a sharp dip in the TA phonon dispersion curve at a high-symmetry point of the Brillouin zone and (ii) the existence of a particular type of defect. In the case of $Pb_3(PO_4)_2$, at least the first condition is satisfied by the existence of the soft phonon mode at L point of the rhombohedral Brillouin zone.

Later, the MLR model has been generalized to be applicable to systems other than bcc alloys. Fuchizaki and Yamada[4] investigated thermodynamical properties of a system which is characterized by (i) the existence of weakly first-order phase transition and (ii) the existence of strong coupling between the order parameter and the bulk strains. They argued that at a weakly first-order phase transition, the "embryonic fluctuations," which are essentially short-range order of the LT structure coherently embedded on the lattice of the HT phase will be thermally excited. Then, the diffraction pattern was calculated assuming random distribution of these embryonic fluctuations. The pattern clearly reproduced the ghost lattice behavior. Then it has been shown that the ghost lattice behavior is reproduced in the calculated diffraction pattern assuming a random distribution of these embryonic fluctuations.

Evidently, $Pb_3(PO_4)_2$ satisfies the above two conditions by taking the order parameter to be the L-zone-boundary mode, which couples to the strain components $e_{11} - e_{22}$ and e_{12}.[20] Moreover, the numerical calculation by Fuchizaki and Yamada showed that just above T_c, the precursor reflection tends to split into two peaks. Our neutron mapping results (Fig. 11) revealed in fact a splitting into doublet which seems to support such a theoretical prediction.[21]

Based on these considerations the physical picture of the ferroelastic phase transition in $Pb_3(PO_4)_2$ is as follows. At higher temperatures, embryonic fluctuations are excited by thermal activation. Consequently, the precursor reflections appear at the ghost lattice points. At the same time, the anomalous thermal expansion of the cell parameters takes place via the strong coupling between the order parameter and the bulk strain. The embryonic fluctuations have a finite size; these characteristics explain the broadening of the precursor reflections as evidenced by neutron and X-ray-scattering experiments. Because of the layerlike structure, the correlation length of fluctuations develops predominantly within the monoclinic b-c plane than in the perpendicular direction.

As the temperature is lowered down to T_c the embryo size becomes progressively enlarged and long lived. Eventually, below T_c, the ferroelastic ordering of the lattice becomes long range and static. Consequently, the precursor reflections become elastic sharp superstructure peaks.

IV. CONCLUSION

This study has shown that the various anomalies occurring at the critical regime of the ferroelastic phase transition of lead phosphate could be satisfactorily interpreted in the framework of the embryonic fluctuation model. Up to now, experimental proofs of embryonic fluctuations have only been found in the premartensitic regime of metals and alloys. Lead phosphate is, to our knowledge, an example of a nonmetallic crystal displaying premartensitic phenomena. We believe that these phenomena are in fact quite general and could be observed in many other compounds undergoing ferroelastic transition, though in many cases it might be difficult to be evidenced, since it requires very high-resolution measurements to detect the ghost lattice effect.

ACKNOWLEDGMENTS

J.M.K. wishes to thank the financial support from the Yamada Science Foundation for his stay in Japan. He is also thankful to J. C. Toledano for giving him the single crystals prepared by J. Aubree. The Laboratoire de Chimie-Physique du Solide is Unité Associée au CNRS No. 453.

[1] M. B. Salamon, M. E. Meichle, and C. M. Wayman, Phys. Rev. B **31**, 7306 (1985).

[2] Y. Yamada, Y. Noda, and M. Takimoto, Solid State Commun. **55**, 1003 (1985).

[3] Y. Noda, M. Takimoto, T. Nakagawa, and Y. Yamada, Metall. Trans. **19a**, 267 (1988).

[4] K. Fuchizaki and Y. Yamada, Phys. Rev. B **40**, 4740 (1989).

[5] J. M. Kiat, Y. Yamada, G. Chevrier, Y. Uesu, P. Boutrouille,

and G. Calvarin, J. Phys. C **4**, 4915 (1992).
[6]C. Joffrin, J. P. Benoit, L. Deschamp, and M. Lambert, J. Phys. (Paris) **38**, 205 (1977).
[7]C. Joffrin, J. P. Benoit, R. Currat, and M. Lambert, J. Phys. (Paris) **38**, 205 (1979).
[8]J. P. Benoit, B. Hennion, and M. Lambert, Phase Trans. **2**, 102 (1981).
[9]Y. Luspin, J. L. Servoin, and F. Gervais, J. Chem. Solids **40**, 661 (1978).
[10]I. Barbur, S. Simon, I. Ardelan, L. Stanescu, and G. Cristea, Rev. Roum. Phys. **33**, 1139 (1988).
[11]C. Manolikas, G. Van Tendeloo, and S. Amelinckx, Solid State Commun. **60**, 749 (1986).
[12]C. N. W. Darlington, Phase Trans. **3**, 283 (1983).
[13]J. Torres, Ph.D. thesis, Université de Paris VI, 1981 (unpublished).
[14]J. Torres, Ferroelectrics **26**, 665 (1980).
[15]D. M. C. Guimaraes, Phase Trans. **1**, 143 (1979).
[16]S. M. Shapiro, Y. Noda, Y. Fujii, and Y. Yamada, Phys. Rev. B **30**, 4314 (1984).
[17]W. Lin, H. Spalt, and B. W. Batterman, Phys. Rev. B **13**, 5158 (1976).
[18]H. G. Smith, N. Wakabayashi, W. P. Crummett, and R. M. Nicklow, Phys. Rev. Lett. **24**, 1612 (1980).
[19]G. H. Lander, J. Magn. Magn. Mater. **29**, 271 (1982).
[20]J. Torres, Phys. Status Solidi B **71**, 141 (1975).
[21]The reason why this splitting could not be observed in the x-ray experiments is not clear. It is not a problem of bad resolution as it is about the same as in the neutron experiment nor can it arise from high-order comtamination, as we used filters. It is probably to be related to the difference in the diffracting geometry: The neutron experiments deal with the bulk of the sample whereas the x-ray experiments (Bragg-Brentano reflection geometry) involve the surface of the sample where relaxation of stresses is known to occur.